I.e. each point in J_R is the limit of a sequence of points from P. If x_0 is an attractive fixed point we consider its *basin of attraction*

$$A(x_0)=\{x\in\overline{\mathbb{C}}: R^k(x)\to x_0 \text{ as } k\to\infty\};$$

$A(x_0)$ collects all points x whose forward orbits $Or^+(x)$ approach x_0. This set includes, of course, the inverse orbit of x_0, $Or^-(x_0)$. If γ is an attractive cycle of period n, then each of the fixed points $R^i(x_0)$, $i=0,\ldots,n-1$, of R^n have their basins and $A(\gamma)$ is simply the union of these basins.
We now list a first set of fundamental results about J_R from [Ju], [Fa]:

Fundamental Properties of Julia Sets

(2.2) $J_R\neq\emptyset$ and contains more than countably many points.

(2.3) The Julia sets of R and R^k, $k=1,2,\ldots$, are identical.

(2.4) $R(J_R)=J_R=R^{-1}(J_R)$.

(2.5) For any $x\in J_R$ the inverse orbit $Or^-(x)$ is dense in J_R.

(2.6) If γ is an attractive cycle of R, then $A(\gamma)\subset F_R=\overline{\mathbb{C}}\setminus J_R$ and $\partial A(\gamma)=J_R$.

(Here $\partial A(\gamma)$ denotes the boundary of $A(\gamma)$, i.e. $x\in\partial A(\gamma)$ provided $x\notin A(\gamma)$ but x is an accumulation point of a sequence with elements from $A(\gamma)$.) Figures 3, 4, 10 and Maps 3–10, 18, 20, 22, 24, 25, 61–66, 75–78, 89–98 are examples of Julia sets bounding two, three or even four different basins of attraction of attractive fixed points.
Further results on Julia sets are:

(2.7) If the Julia set has interior points (i.e. there are points $\bar{x}\in J_R$ such that for some $\varepsilon>0$ $\{x: |x-\bar{x}|<\varepsilon\}\subset J_R$) then $J_R=\overline{\mathbb{C}}$.

This situation appears to be rare, but the mapping $R(x)=((x-2)/x)^2$ is an example. (See Special Section 3.)

(2.8) If $\bar{x}\in J_R$, $\varepsilon>0$, and $J^*=\{x\in J_R: |x-\bar{x}|<\varepsilon\}$, then there is an integer n such that $R^n(J^*)=J_R$.

A number of comments seem to be in order. Property (2.2) implies that every rational map has a considerable repertoire of repelling periodic points. According to (2.4) the Julia set is invariant under R, and the dynamics on J_R is chaotic in some sense as a result of (2.1). Property (2.5) suggests a numerical way to generate pictures of J_R. Unfortunately the inverse orbit of a point $\bar{x}\in J_R$ usually does not distribute uniformly over the Julia set. (See Fig. 27 for the distribution of $Or^-(\bar{x})$ for a typical Julia set.) Therefore sophisticated algorithms are necessary to decide which branches of the tree-like structure in $Or^-(\bar{x})$ should be chosen for an effective picture generation. Such algorithms have been developed and used for our images. Property (2.6) immediately suggests that J_R must be a fractal in many cases. For example, if R has more than two attractive fixed points $a, b, c, \ldots$ then (2.6) implies

$$\partial A(a)=J_R=\partial A(b)=J_R=\partial A(c)=\ldots$$

i.e. the boundaries of all basins of attraction coincide. For example, if R has 3 or 4 attractive fixed points, then J_R is a set of 3-corner-points or 4-corner-points with regard to the respective basins of attraction.

The Dynamics Near Indifferent Periodic Points

Since attractive periodic points belong to F_R, and repelling periodic points belong to J_R, we may ask about *indifferent points*. This question is in fact very delicate and still not completely understood. Without loss of generality we may assume that $R(0)=0$ and $R'(0)=\lambda$ with $|\lambda|=1$, i.e. $\lambda=\exp(2\pi i\alpha)$ with $\alpha\in[0,1]$. Let

$$R(x)=\lambda x+a_2x^2+a_3x^3+\ldots$$

be the power series for R. There are two types of indifferent points: the fixed point 0 is called *rationally* indifferent if α is a rational number; it is called *irrationally indifferent* if α is an irrational number. A rationally indifferent fixed point (or cycle) is also called *parabolic*.
It was known to *Julia* and *Fatou* that

(2.9) $x_0\in J_R$ if x_0 is a parabolic periodic point of R.

Moreover, they knew that in this case $A(\gamma)\neq\emptyset$, $\gamma=\{x_0, R(x_0),\ldots,R^{n-1}(x_0)\}$ and $\gamma\subset\partial A(\gamma)$. Figures 6, 8, and 9 illustrate this situation.
A more comprehensive characterization of indifferent points requires a closer look into the *dynamics* of R near $R(0)=0$. The following result from [Cam] accounts for the parabolic case:

The Parabolic Case

(2.10) Let $\lambda=R'(0)$, $\lambda^n=1$ and $\lambda^k\neq1$ for $0<k<n$. Then either R^n is the identity or there exists a homeomorphism h (defined in a neighborhood of 0) with $h(0)=0$ and

$$h\circ R\circ h^{-1}(x)=\lambda x(1+x^{kn})$$

for some $k\geq1$.

Siegel Disks

The irrational case is considerably more difficult. We need the concept of stability:

(2.11) $R(0)=0$ is called *stable* if for any neighborhood U of 0 there exists a neighborhood V of 0 such that $V\subset U$ and

$$R^k(V)\subset U$$

for any $k\geq1$.

Attractive fixed points are obviously stable. To describe the stability of indifferent fixed points we use a result of J. Moser and C.L. Siegel [MS]:

(2.12) Let $R(x)=\lambda x+a_2x^2+\ldots$, $|\lambda|=1$ and $\lambda^n\neq 1$ for any $n\in\mathbb{N}$. Then 0 is a stable fixed point if and only if the functional equation

$$\Phi(\lambda x)=R(\Phi(x))$$

has an analytic solution in a neighborhood of 0.

The above functional equation is called Schröder's equation in honor of E. Schröder who studied its solvability in 1871. What does it actually mean? Assume that it holds for a $\lambda=\exp(2\pi i\alpha)$, then

$$\lambda x=\Phi^{-1}(R(\Phi(x))).$$

I.e. R is *locally equivalent* (or conjugate) to a *rotation* by $2\pi\alpha$. To solve Schröder's equation one tries an Ansatz for Φ: let $R(x)=\lambda x+a_2x^2+\ldots$. If

(2.13) $\Phi(x)=x+b_2x^2+\ldots$

then (2.12) yields

$$(2.14)\quad \sum_{i=2}^{\infty}(\lambda^i-\lambda)b_ix^i=\sum_{i=2}^{\infty}a_i\Big(x+\sum_{k=2}^{\infty}b_kx^k\Big)^i$$

and formally one can obtain the b_i, $i=2,3,\ldots$, by comparing coefficients. The problem then however, is to show convergence. Obviously, this method does not work if λ is a root of unity, i.e. $\lambda=\exp(2\pi ip/q)$. When α is irrational, then (2.14) is called a *small divisor problem*. In 1917 G.A. Pfeifer gave an example where Schröder's series (2.13) does not converge. In 1938 H. Cremer was able to provide a whole class of examples for which (2.13) diverges:

(2.15) $\{\lambda: |\lambda|=1 \text{ and } \liminf|\lambda^n-1|^{1/n}=0\}$.

Then in 1942 C.L. Siegel [Si] in a groundbreaking work (which eventually became all important in the Kolmogoroff-Arnold-Moser theory) showed that Schröder's series actually converges provided that α satisfies a diophantine condition ($\lambda=\exp(2\pi i\alpha)$):

(2.16) There exist $\varepsilon>0$ and $\mu>0$ such that

$$|\alpha-\frac{m}{n}|>\frac{\varepsilon}{n^{\mu}}$$

for all integers m and positive integers n.

The condition on α loosely says *α is badly approximated by rational numbers*. If we write the irrational number α in its continued fraction expansion, we can make this statement precise. Let $\alpha=(a_0, a_1, a_2, \ldots)$ be this expansion, i.e., $a_k\in\mathbb{N}$ and

$$\alpha=a_0+\cfrac{1}{a_1+\cfrac{1}{a_2+\cfrac{1}{a_3+\ddots}}}$$

Then set $\frac{p_n}{q_n}=(a_0, a_1, \ldots, a_n, 0, 0, 0, \ldots)$. These numbers are the best rational approximants to α and it is well known that

$$\frac{1}{(a_{n+1}+2)q_n^2}<|\alpha-\frac{p_n}{q_n}|<\frac{1}{a_{n+1}q_n^2}.$$

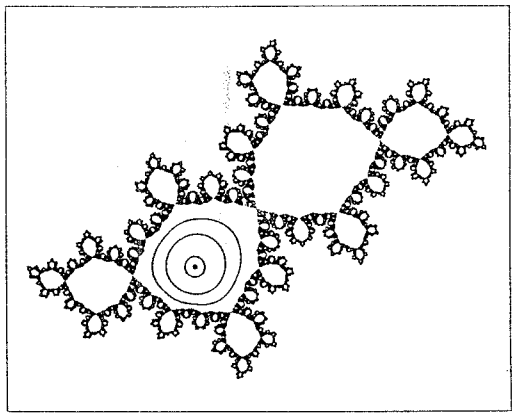

Fig. 22. Siegel disk around the irrationally indifferent fixed point $x_0=0$ for the mapping $x\mapsto x^2+\lambda x$, $\lambda=e^{2\pi i\alpha}$, $\alpha=(\sqrt{5}-1)/2$. On the invariant curves (3 are shown) the dynamics is equivalent to a rotation about the angle α

(Here best means that no rational p/q with $q\leqslant q_n$ is closer to α than $\frac{p_n}{q_n}$.)

Hence, for example, if the a_k's stay bounded, one can verify the diophantine condition in (2.16). It is known and not difficult to prove that any algebraic number of degree 2 has such a continued fraction expansion and thus such numbers α (and in fact all algebraic numbers) satisfy the diophantine condition. A prominent example is the golden mean

$$\alpha=(\sqrt{5}-1)/2,\quad \alpha=(0, 1, 1, 1, \ldots).$$

It is known that the set of $\alpha\in[0, 1]$, for which Siegel's condition is satisfied is a set of full measure. If Schröder's series (2.13) converges, one says that R is linearizable in 0. The maximal domain $D(0)$, containing $R(0)=0$, in which $\Phi(\lambda x)=R(\Phi(x))$ holds is called a Siegel disk. Maps 22 and 25 show an example from the quadratic family $x\mapsto x^2+c$. These color maps show a Siegel disk, its preimages under R, and the basin of attraction of ∞. The coloring in Map 25 reveals the invariant circles to which the dynamics near the irrationally indifferent fixed point is confined. Figure 22 shows such a fixed point, some invariant curves and the Julia set.

In this example we observe that the critical point $x_c=-e^{2\pi i\alpha}/2$ belongs to the Julia set confirming a recent result of M. Herman (see also Special Section 3). Also note that

(2.17) $x_0\in F_R$, if x_0 is the center of a Siegel disk.

In 1972 H. Rüßmann was able to extend Siegel's result even to certain Liouville numbers. (Liouville numbers λ are very close to rational numbers.) The

exact condition on α for which Schröder's series converges is an open and apparently very deep problem. Consequently, one cannot as of yet always determine if a given irrationally indifferent fixed point is in either the Julia set or the Fatou set.
If $R(x)=x^2+\lambda x$, then of course for every $\lambda \in S^1$ we have that $x_0=0$ is an indifferent fixed point. Imagine that λ is varying on S^1. Then, no matter how small the change is, the dynamics near $x_0=0$ will undergo most dramatic changes. This is because any change of λ will always result in infinitely many parabolic and Siegel disk cases.

The Hausdorff Dimension

According to B.B.Mandelbrot a set X is called a *fractal* provided its *Hausdorff dimension* $h(X)$ is not an integer. Intuitively $h(X)$ measures the growth of the number of sets of diameter ε needed to cover X, when $\varepsilon \to 0$. More precisely, if $X \subset \mathbb{R}^m$, let $n(\varepsilon)$ be the number of m-dimensional balls of diameter ε needed to cover X. Then if $n(\varepsilon)$ increases like

(2.18) $\quad n(\varepsilon) \propto \varepsilon^{-D}$ as $\varepsilon \to 0$,

one says that X has Hausdorff dimension D. It is not hard to show that if C is the familiar Cantor set, then

$$h(C)=\log 2/\log 3.$$

A rigorous definition for $h(X)$ proceeds as follows: let X be a subset of a metric space and let $d>0$. The d-dimensional *outer measure* $m_d(X)$ is obtained from

(2.19)
$$\begin{cases} m_d(X,\varepsilon)=\inf\{\sum_{i\in I} (\operatorname{diam} S_i)^d\}, \text{ where the inf is over all finite coverings} \\ \text{of } X \text{ by sets } S_i \text{ with diameter less than } \varepsilon>0. \\ m_d(X)=\lim_{\varepsilon \to 0} m_d(X,\varepsilon). \end{cases}$$

Now $m_d(X)$, depending on the choice of d, may be finite or infinite. F.Hausdorff showed in 1919 that there is a unique $d=d^*$ at which $m_d(X)$ changes from infinite to finite as d increases. This then leads to the definition

(2.20) $\quad h(X)=\sup\{d \in \mathbb{R}_+ : m_d(X)=\infty\}$.

(See [Fal] for more details and examples.)
Recently, D.Ruelle [Ru2] obtained the following remarkable result: let J_c be the Julia set for $x \mapsto x^2+c$. Then for $|c| \ll 1$ one has

(2.21) $\quad h(J_c)=1+\dfrac{|c|^2}{4 \log 2}+$ *higher order terms.*

It is also known (see [Bro]) that for c small J_c is a Jordan curve (i.e. the homeomorphic image of the unit circle). In fact J_c is a Jordan curve for any c in the main part (the cardioid) of the Mandelbrot set. Though Julia sets are typically of fractal nature, almost nothing is known about their Hausdorff dimension. Ruelle's result seems to be the first sharp result in that direction.

Julia Sets for Transcendental Maps

In Section 6 we will continue to discuss some special classes of Julia sets, namely those for Newton's method in the complex plane. In Section 7 we compare our results from Section 6 with some first findings for Julia-like sets obtained from Newton's method for real equations. Our experiments there reveal structures which look quite different from the baroque structures which we have seen so far for rational mappings in the complex plane. One is tempted to attribute this apparent baroqueness to the underlying complex analytic structure. This is a little premature, however, as the following example indicates. R.Devaney [De] recently has studied some first examples of transcendental mappings, as for example

(2.22) $\quad E_\lambda(x)=\lambda \exp(x)$,
(2.23) $\quad S_\lambda(x)=\lambda \sin(x)$,

$\lambda \in \mathbb{C}$, in $\overline{\mathbb{C}}$. He obtained some very remarkable results, a few of which we want to include here. Defining the Julia set for E_λ (or S_λ) according to (2.1), i.e.

(2.24) $\quad J_\lambda=$ closure $\{x \in \mathbb{C}: x$ is a periodic repelling point of E_λ (resp. $S_\lambda)\}$

then a first result is

(2.25) $\quad J_\lambda=$ closure $\{x \in \mathbb{C}: E_\lambda^n(x) \to \infty$ (resp. $S_\lambda^n(x) \to \infty$) as $n \to \infty\}$.

Note that there is a distinctive change in the behavior of E_λ, for example, as λ passes through $1/e$ along the real axis (see Fig.23).
If $\lambda<1/e$ there is an attractive fixed point Q_λ and a repelling fixed point P_λ, while if $\lambda>1/e$ there is none. Also, if $\lambda<1/e$ one has apparently that

(2.26) $\quad \{x \in \mathbb{R} : x \geq P_\lambda\} \subset J_\lambda$.

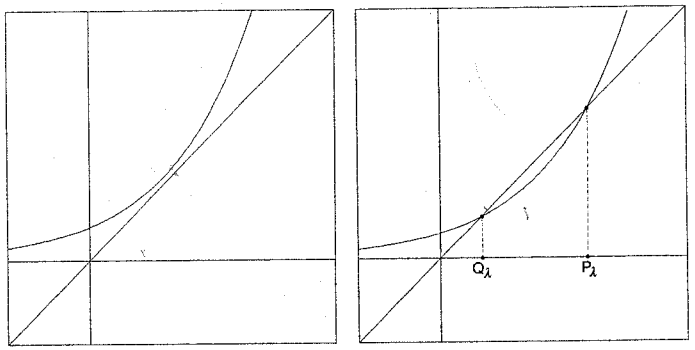

Fig. 23. The graph of $x \mapsto \lambda \exp(x)$, $x \in \mathbb{R}$, $\lambda \in \mathbb{R}$. Left: $\lambda>1/e$; right: $\lambda<1/e$

Devaney calls this ray a hair. It turns out to be crucial in the description of J_λ. One of his main results is:

(2.27) $\begin{cases} \text{If } \lambda > 1/e, \text{ then } J_\lambda = \mathbb{C}. \\ \text{If } \lambda < 1/e, \text{ then } J_\lambda \text{ is a nowhere dense Cantor set of curves which form the boundary of a single basin of attraction.} \end{cases}$

Thus, as λ increases and passes through $1/e$, J_λ experiences an explosion. Pictures of Julia sets for this family are quite difficult to obtain and we refer to [De] for a sketch of a picture.
Inspired by Mandelbrot's work (see Special Section 4) Devaney also discusses a bifurcation set for E_λ in the λ-plane:

(2.28) $B = \{\lambda \in \mathbb{C}: J_\lambda = \mathbb{C}\}$ and
(2.29) $C = \mathbb{C} \setminus B$.

He shows that the interior of C contains components which are indexed by the period of attractive periodic points. Figure 24 gives a sketch of B in black.
This study is based on another result of Devaney:

(2.30) If $E_\lambda^n(0) \to \infty$, then $J_\lambda = \mathbb{C}$.

This result suggests to color a point in the λ-plane black if $|E_\lambda^n(0)| \geq M$, $M \gg 1$, for some $n < N_{\max}$. The picture in Fig. 24 has to be interpreted with some care. For example, the white set contains points like $\lambda = 2k\pi i$. I.e., $E_\lambda^2(0) = E_\lambda(\lambda) = \lambda$. In general:

(2.31) If 0 is preperiodic (i.e. $E_\lambda^n(0)$ is periodic for some $n \geq 1$), then $J_\lambda = \mathbb{C}$.

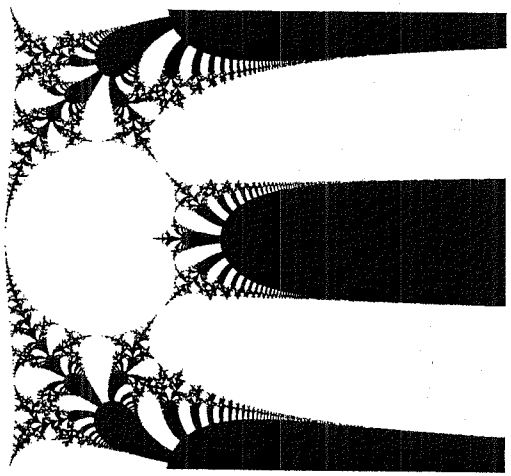

Fig. 24. Mandelbrot-like set for E_λ (the solid black domains are an artifact of the low iterational resolution $N_{max} = 90$)

For each λ such that $|E_\lambda^n(0)| \geq M$ for some $n \leq N_{\max}$, there is a first n of this kind. This associates an index to each such λ, which can be used to determine a color in a *Color Look Up Table* to generate beautiful color graphics.
Comparing Devaney's results with pictures of other Julia sets, they seem to share more properties with the Julia-like sets in Section 7 than with Julia sets of rational mappings. For example, J_λ is not locally connected, like many of the Julia-like sets in Section 7. Also we have found that the Julia-like sets there typically contain "hairs" like (2.26). ($X \subset \mathbb{C}$ is called locally connected if for U open in $\mathbb{C}$ and $U \cap X \neq \emptyset$ one has that for any $x \in U \cap X$ there is a neighborhood $V \subset U$, $x \in V$, such that $V \cap X$ is connected.)

Generating Pictures of Julia Sets

There are essentially two different ways to generate pictures of Julia sets. One is based on (2.5) and the other builds on (2.6). None of the methods has an advantage over the other. In some cases the first method is very successful while the second is quite unsatisfactory, and vice versa. Then there is a large class of cases in which both work fine. But there is also a large class of Julia sets for which it is very difficult if not impossible to generate satisfactory pictures. This class contains Julia sets bounding parabolic domains, i.e. the mapping has a parabolic periodic point.

The Inverse Iteration Method (IIM)

Given a rational mapping R and a periodic repeller $\bar{x} \in J_R$, property (2.5) suggests to compute

(2.32) $J_R^n = \{x \in \mathbb{C}: R^k(x) = \bar{x} \text{ for some } k \leq n\}$.

Since $J_R = \text{closure}\left(\bigcup_{n \geq 0} J_R^n\right)$ one expects that plotting J_R^n for a sufficiently large n should give a good picture of J_R. Indeed, if J_R^n is uniformly distributed over J_R, then this method generates a satisfactory picture of J_R. Intuitively speaking, we say that the inverse orbit $Or^-(\bar{x})$ distributes uniformly provided the number of points in ($\varepsilon > 0$, ε small)

$$J_R^n \cap D(x,\varepsilon), \qquad (x \in J_R,\ D(x,\varepsilon) = \{y: |y-x| < \varepsilon\})$$

is essentially independent of x for large n. Unfortunately, this is not typical. More typically one has neighborhoods on J_R which are visited only extremely rarely. In these cases the direct IIM is inappropriate. Recall that the number of elements in J_R^n grows like d^n, where d is the degree of R. Figure 25 shows a typical situation.
The shortcomings of this experiment become apparent if one compares Fig. 25 with Map 18, where the red domain identifies the basin of attraction of an attractive cycle of period 11 and the Julia set is its boundary. Figures 26 and 27 show another Julia set from the quadratic family $R(x) = x^2 + c$ together with a demography of J_R^n based on a covering of J_R.
In these experiments, J_R is put on a square lattice in $\mathbb{C}$ with small mesh size. The number of points from J_R^n in each little box of that lattice is measured and

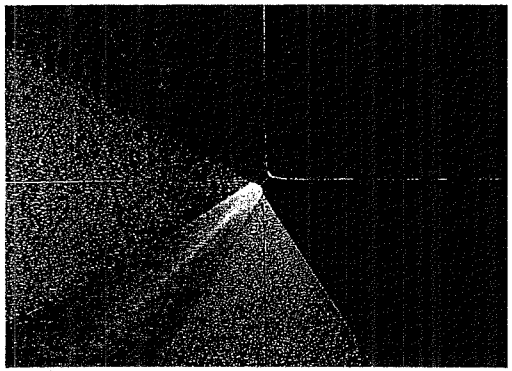

Map 19

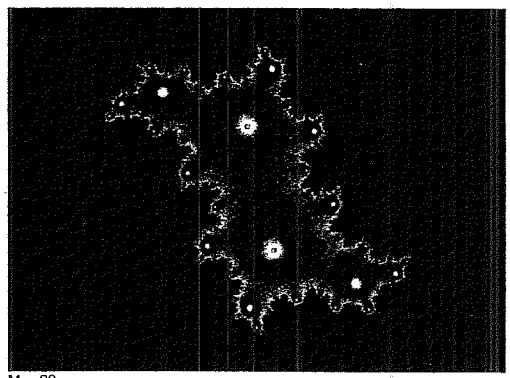

Map 20

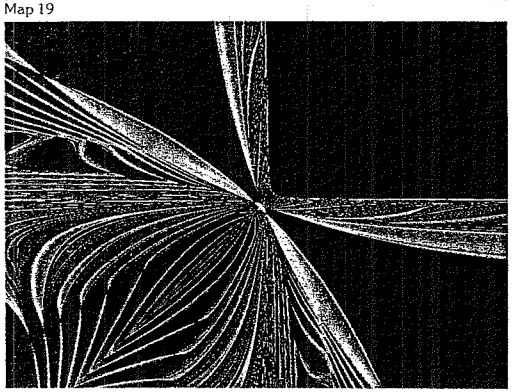

Map 21

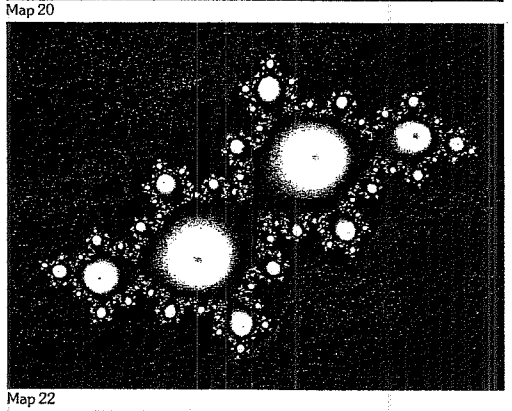

Map 22

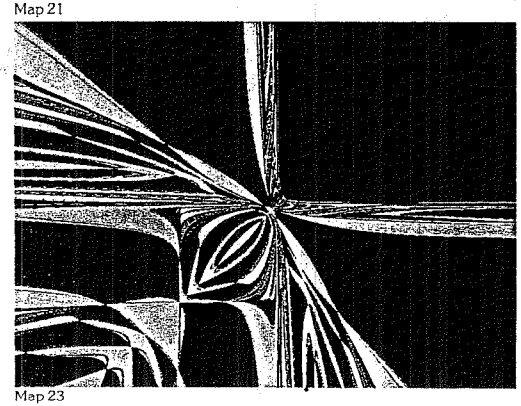

Map 23

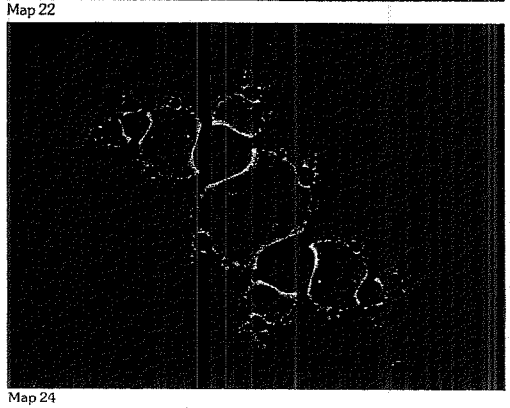

Map 24

3 Sullivan's Classification and Critical Points

From the complexity of the computer experimental results it may appear impossible to understand the *global* dynamics of a given rational map R. But Julia and Fatou already knew that many of its qualitative aspects are intimately linked to the dynamics of the critical points of R.

(3.1) A number $c \in \overline{\mathbb{C}}$ is called a *critical value* of R if the equation $R(x)-c=0$ has a degenerate zero, i.e. a zero of multiplicity greater than 1. Any such zero is called a *critical point*. Finite critical points are obtained as solutions to $R'(x)=0$.

To report on the remarkable results of D. Sullivan (1983) [Su], we need the concept of an immediate basin of attraction:
Let x_0 be an attractive or rationally indifferent fixed point of R and let $A(x_0)$ denote its basin of attraction. Then the *immediate basin of attraction* $A^*(x_0)$ is the connected component of $A(x_0)$ containing x_0. In Fig. 3 $A^*(x_0)=A(x_0)$ which is one of the reasons why J_c is in fact a Jordan curve in that example (i.e. a homeomorphic image of the unit circle). In Fig. 6 we see a parabolic fixed point with the shaded region being $A^*(x_0)$. In Fig's. 53 g–j we have typical examples of attractive fixed points ($x_0=1$) with $A^*(x_0) \neq A(x_0)$ (see also Map 10). It is a fact that $A^*(x_0)$ is either simply connected (no holes) or has infinite connectivity (infinitely many holes). Maps 7–9 illustrate the latter situation: the white specks designate holes in a blow up of a part of $A^*(x_0)$.
We can also define the immediate basin of attraction of a periodic orbit $\gamma=\{x_0, R(x_0), R^2(x_0), \ldots, R^{n-1}(x_0)\}$ of period n (i.e. $R^n(x_0)=x_0$) which is attractive or rationally indifferent. First let $A^*(x,S)$ denote the immediate basin of a fixed point x for any mapping S. Then for periodic orbits of period n we set

$$(3.2) \quad A^*(\gamma)=\bigcup_{k=0}^{n-1} A^*(R^k(x_0), R^n).$$

In Fig. 4 the shaded region illustrates $A^*(\gamma)$ of an attractive 3-cycle. Similarly, if $\gamma=\{x_0, R(x_0), \ldots, R^{n-1}(x_0)\}$ is a periodic orbit of period n, which is irrationally indifferent and such that R^n is linearizable in x_0, we set

$$(3.3) \quad D(\gamma)=\bigcup_{k=0}^{n-1} R^k(D_0),$$

where D_0 is the Siegel disk of x_0 for R^n. (In case x_0 is a fixed point, γ is simply the set $\{x_0\}$.)
We can now state Sullivan's results [Su] which completely characterize the Fatou set F_R:

No Wandering Domains

(3.4) The Fatou set $F_R = \overline{\mathbb{C}} \setminus J_R$ has countably many connected components. If X_0 is such a component, then X_0 is eventually periodic, i.e. for some k one has that $R^k(X_0)$ is a periodic component of F_R. In short: R has *no wandering domains.*

This answers one of the major problems left open in the work of Julia and Fatou. (Sullivan's proof uses Teichmüller theory and the theory of Fuchsian and Kleinian groups.) Building on fundamental results of Julia and Fatou, a complete classification is thereby possible.

Classification into Five Types

(3.5) Let X_0 be a periodic connected component of F_R of period n, and

$$\Gamma = \bigcup_{k=0}^{n-1} R^k(X_0)$$

the associated cycle*. Then Γ is one of the following:

(A) An immediate basin $A^*(\gamma)$ associated with a superattractive cycle γ
(B) An immediate basin $A^*(\gamma)$ associated with an attractive cycle γ.
(C) An immediate basin $A^*(\gamma)$ associated with a parabolic cycle γ.
(D) A collection of Siegel disks $D(\gamma)$ associated with an irrationally indifferent cycle γ [see (3.3)].
(E) A collection of Herman rings

$$H = \bigcup_{k=0}^{n-1} R^k(H_0).$$

The last alternative was discovered a few years ago by M. Herman. It is not associated with a periodic point but it is similar to case D: On H_0, R^n is analytically equivalent to an irrational rotation of the standard annulus.
Each of the cases (A)–(E) is furthermore characterized by critical points:

Detection by Critical Points

(3.6) In cases (A)–(C) $A^*(\gamma)$ contains at least one critical point. In cases (D) and (E) the boundary of $D(\gamma)$ or H is in the closure of the forward orbit of a critical point (i.e. there is a critical point x_c such that $Or^+(x_c)$ gets arbitrarily close to $\partial D(\gamma)$ or ∂H).

Now if d is the degree of the rational function R, it is easy to see that R has at most $2d-2$ critical points. (If R is the quotient of two relatively prime polynomials, then the degree of R is the maximum of the degrees of these.) Thus R

* Note that we use the term cycle for Γ although Γ may not contain any periodic point (e.g. in case (E)).

can only have finitely many cycles of type (A)–(E). It is not known whether $2d-2$ is an upper bound. It is conjectured that the boundary of $D(\gamma)$ (see (C)) always contains a critical value. In fact M. Herman was able to support this by showing that it is true for $R(x) = z^m + a$, $m = 2, 3, \ldots$ $a \in \mathbb{C}$.
As a remarkable application of (3.6) we mention the following example from [MSS]: Let $R(x) = ((x-2)/x)^2$, then $J_R = \overline{\mathbb{C}}$! To see this, note that the critical points of R are $\{2, 0\}$ and that $2 \mapsto 0 \mapsto \infty \mapsto 1 \mapsto 1$ and $R'(1) = -4$. Thus $\overline{\mathbb{C}} \setminus J_R$ must be the empty set, because otherwise (3.5) and (3.6) would apply.

4 The Mandelbrot Set

For polynomials of second order, $p(x)=a_2x^2+a_1x+a_0$, an almost complete classification of the corresponding Julia sets can be given in terms of the Mandelbrot set. First note that $p(x)$ is conjugate to $p_c(z)=z^2+c$ by means of the coordinate transformation $x \mapsto z=a_2x+a_1/2$, with $c=a_0a_2-\frac{a_1}{2}\left(1-\frac{a_1}{2}\right)$.

This transformation shifts the finite critical point $x=-a_1/2a_2$ into the origin. It is thus sufficient to study the nature of the Julia sets of $p_c(z)$.

The point ∞ is a superattractive fixed point of the mapping $z \mapsto p_c(z)$. The Julia set J_c, for given $c\in\mathbb{C}$, can therefore be characterized as $J_c=\partial A(\infty)$. From the theory of Julia and Fatou it follows that J_c is either connected or a Cantor set [Bl]. This distinction is reflected in the definition of the Mandelbrot set:

(4.1) $M=\{c\in\mathbb{C}: J_c \text{ is connected}\}$.

Figures 3, 4, 6–10, 12 and 14 are examples of connected Julia sets whereas Figs. 11, 13 and 15 show Julia sets with Cantor set structure. Among the connected Julia sets there are those which enclose an interior and others, like Fig. 12, which are dendrites without an inner region.

To compute M, B.B. Mandelbrot employed the powerful results of Julia and Fatou according to which the main dynamical features of a rational mapping can be inferred from the forward orbits of its critical points (see special Section 3): Any attractive or rationally indifferent cycle has in its domain of attraction at least one critical point. But $p_c(z)$ has only two critical points, $z=0$ and ∞, which are independent of c. The point ∞ is already an attractive fixed point, so only 0 remains as an interesting critical point to study. By choosing $c=1$, e.g., we see that there are values of c for which $0\in A(\infty)$, since $0 \mapsto 1 \mapsto 2 \mapsto 5 \mapsto 26 \mapsto 677 \mapsto \ldots$. In these cases there cannot be another attractor besides ∞. On the other hand, as the case $c=0$ shows, there are also c such that there is another attractor: under $p_0(z)=z^2$, the point $z=0$ attracts all z with $|z|<1$, i.e. $J_0=S^1$.

Now according to Julia and Fatou, J_c is connected if and only if $0\notin A(\infty)$, see [Bl], i.e.

(4.2) $M=\{c\in\mathbb{C}: p_c^k(0) \not\to \infty \text{ as } k\to\infty\}$.

This characterization is very suitable for numerical studies. One chooses a lattice of points $c\in\mathbb{C}$ and tests for every such c whether after N iterations the modulus of the sequence $0 \mapsto c \mapsto c^2+c \mapsto \ldots$ is still below a given bound m. (For Fig. 2 we took $N=1000$ and $m=100$.)

A. Douady and J.H. Hubbard [DH1] have found a deep analytic characterization of M. They studied the nature of *filled-in Julia sets* K_c

(4.3) $K_c=\{z\in\mathbb{C}: p_c^k(z) \not\to \infty \text{ as } k\to\infty\}$,

and noticed that for $c\in M$ their complements can be mapped onto the complement of the closed unit disk $\bar{D}$, by means of a conformal mapping φ_c,

(4.4) $\varphi_c: \bar{\mathbb{C}}\setminus K_c \to \bar{\mathbb{C}}\setminus\bar{D}$.

Remarkably, this mapping can be chosen in such a way that

(4.5) $\varphi_c \circ p_c \circ \varphi_c^{-1}=p_0$.

Note that locally φ_c is guaranteed by Boettcher's result (2.34). This identifies M as

(4.6) $M=\{c\in\mathbb{C}: p_c \text{ on } A(\infty) \text{ is equivalent to } z \mapsto z^2\}$.

The conjugation (4.5) is even possible for $c\notin M$, but then it does not hold in all of $A(\infty)$. Nevertheless, it can be extended far enough to hold at the point $z=c$, and by setting

(4.7) $\psi(c):=\varphi_c(c)$,

we have a mapping $\psi: \bar{\mathbb{C}}\setminus M \to \bar{\mathbb{C}}\setminus\bar{D}$ which is a conformal isomorphism. In this way Douady and Hubbard demonstrated that

(4.8) M is a *connected* set

(i.e. M is not contained in the union of two disjoint open nonempty sets). It is still unknown, however, whether M is also *locally connected*, i.e. whether any piece $U\cap M$ of M ($U\subset\mathbb{C}$ open) has the property that for any $z\in U\cap M$ there is a neighborhood $V\subset U$, $z\in V$, such that $V\cap M$ is connected. The difficulty is that one cannot draw on properties of K_c because there are c for which K_c is not locally connected. Nevertheless, it is believed that the local connectedness of M does in fact hold. This would have important consequences one of which is discussed in Special Section 5.

Yet another characterization of M has recently been given by F.v. Haeseler [Ha]. Using the coordinate change $z=1/u$ one first transforms p_c into the rational mapping $R_c(u)=u^2/(1+cu^2)$. The superattractive fixed point for all c is then $u=0$, and in a neighborhood of 0 R_c can be conjugated to R_0 (only for $c\in M$, of course, can this conjugation be extended to the entire basin of attraction $A(0)$). Let $\Phi_c(u)=u+a_2(c)u^2+a_3(c)u^3+\ldots$ be that local conjugation. Then

(4.9) $M=\{c\in\mathbb{C}: |a_k(c)|\leq k,\ k=2,3,\ldots\}$.

This bears an intriguing relationship to the Bieberbach conjecture which was recently proved by L. de Branges [Br]. Let

$S=\{f: D\to\mathbb{C}: f(x)=x+a_2x^2+\ldots, f \text{ analytic and injective}\}$,

where D is the open unit disk; the functions in S are called *schlicht* functions. The Bieberbach conjecture was:

(4.10) If $f\in S$ then $|a_k|\leq k$, $k=2,3,\ldots$.

As a consequence of (4.9) F.v. Haeseler obtained

(4.11) $M\subset\{c\in\mathbb{C}: |c|\leq 2\}$.

Since $c=-2$ belongs to M, the estimate could not be better.

Let us now consider M in more detail. A particularly interesting part of M is

(4.12) $M' = \{c \in \mathbb{C} : p_c \text{ has a finite attractive cycle}\}$.

Since each attractor absorbs a critical point, there can be only one such cycle for each c. It turns out that M′ is an open set with infinitely many connected components. Each component is characterized by the period of the corresponding cycle. The main cardioid, e.g., contains all c for which p_c has a stable fixed point. By computing $\lambda = dp_c/dz$ at the fixed point and imposing the stability condition $|\lambda| < 1$, we find that this comprises the set

(4.13) $M_1' = \{c \in \mathbb{C} : c = \frac{\lambda}{2}(1 - \frac{\lambda}{2}), |\lambda| < 1\}$.

To characterize the components W of M' further, Douady and Hubbard consider the eigenvalue $\rho_W(c)$ of the attractive cycle that exists for $c \in W$. They show that the mapping

(4.14) $\rho_W : W \to D$

is a conformal isomorphism. Thus each component W has a well-defined *center* c_W whose corresponding attractive cycle is superstable, $\rho_W(c_W) = 0$. Let $\{z_1, z_2, \ldots, z_k\}$ be the attractor for a given $c \in W$. Then $\rho_W(c) = 2^k \prod_i z_i$. If this is to be zero, the critical point $z = 0$ must belong to the cycle. The centers of components with k-periodic attractors are therefore given by

(4.15) $p_c^k(0) = 0$.

This equation is of degree 2^{k-1} in c so that there may be up to 2^{k-1} components with k-periodic attractors. We give a list of centers with periods up to 4.

(4.16) $k = 1$: $c = 0$; the corresponding component of M' is M_1' as given in (4.13).

(4.17) $k = 2$: $c^2 + c = 0$ with 2 solutions $c = 0$ and $c = -1$. The center $c = 0$ has already been obtained for $k = 1$. There is thus one component $W = M_2'$ with stable orbits of period 2; it is the disk of radius 1/4 around $c = -1$.

(4.18) $k = 3$: $(c^2 + c)^2 + c = 0$. Ignoring the solution $c = 0$, it remains to solve $c^3 + 2c^2 + c + 1 = 0$. The real solution $c = -1.7549$ is the center of the secondary Mandelbrot set shown in Map 32 while the two complex solutions $c = -0.1226 \pm 0.7449i$ are the centers of the most prominent buds on M_1'.

(4.19) $k = 4$: Two of the eight solutions of $p^4(0) = 0$ have already been obtained with $k = 2$. Of the remaining 6, two are on the real axis: $c = -1.3107$ is the center of the bud that develops from M_2' by period doubling, $c = -1.9408$ is from a satellite near the tip of the main antenna. The four complex solutions are $c = 0.282 \pm 0.530i$, corresponding to buds on M_1', and $c = -0.1565 \pm 1.0323i$ one of which is the center of the Mandelbrot figure in the cover picture of this book.

In addition to the center $c = 0$, we have 15 centers of period 5, and so on. Obviously, by going to higher and higher periods we would find centers closer and closer to the boundary of M.

The mapping (4.14) can be extended to the boundaries of W and D. If $c \in \partial W$ and $\rho_W(c) = \exp(2\pi i\alpha)$, it is said that c is a point of *internal angle* α. The point of internal angle $\alpha = 0$ is called the *root* of W; this is where W buds from another component of M' or, if W is a *primitive* component not budding from another one, the root is the cusp of the cardioid. If $c \in \partial W$ is a point of rational internal angle $\alpha = p/q$, then there is a *satellite* component budding from W at the point c, whose attractive cycles have q times the period of the cycles of W. For example, for $\lambda = \exp(2\pi ip/q)$ in (4.13) we can identify the points on M_1 where satellites are attached. For $p/q = 1/2$ we find $c = -3/4$; the period 3 buds ($p/q = \pm 1/3$) are attached at $c = (-1 \pm 3\sqrt{3}\,i)/8 = -0.1250 \pm 0.6495i$, and period 4 buds grow from $c = 1/4 \pm i/2$. For all these values of c, the mapping p_c has rationally indifferent cycles. Figures 6 and 8 correspond to $p/q = 3/5$ and $1/20$ respectively; for Map 18 we chose $p/q = 1/11$. If, on the other hand, the internal angle is sufficiently irrational in the sense of the diophantine condition (2.16), we find Siegel disks occurring. Fig. 7 and Map 25 derive from $c = \rho_{M_1'}^{-1}(\exp\{2\pi i\alpha\})$, see (4.13), with $\alpha = (\sqrt{5} - 1)/2$.

So far we have discussed the components of M' with their centers and roots. Another conspicuous feature of M are the tips and the branch points of its antennas. For example, the point $c = -2$ is characterized by the critical point being mapped into the repulsive fixed point, $0 \mapsto -2 \mapsto 2 \mapsto 2$. More generally, for the c-values in question, the point $z = 0$ is preperiodic but not periodic; it is eventually drawn into a repulsive cycle.

(4.20) $p_c^n(0) = p_c^{n-k}(0)$, $n \geq 3$, $n - 2 \geq k \geq 1$.

Such c-values are known as Misiurewicz points.

Consider only the simplest cases $n = 3$ and $n = 4$:

(4.21) $n = 3, k = 1$:
$(c^2 + c)^2 + c = c^2 + c$. Discarding the solution $c = 0$ (for which we know that $z = 0$ is itself periodic) we only have $c = -2$, the tip of the main *antenna*.

(4.22) $n = 4, k = 1$:
$((c^2 + c)^2 + c)^2 + c = (c^2 + c)^2 + c$. Again discarding $c = 0$ and also $c = -2$, we obtain three solutions. The real solution $c = -1.54369$ is a "band-merging point" in the analysis of Großmann and Thomae [GT]; the complex solutions $c = -0.22816 \pm 1.11514i$ are perhaps best seen in Map 28, where they are the antenna tips that reach farthest in the imaginary direction.

(4.23) $n = 4, k = 2$:
$((c^2 + c)^2 + c)^2 + c = c^2 + c$. Ignoring the solutions $c = 0, -1, -2$ which have already been discussed, we are left with $c = \pm i$. These c-values mark ends of the side *antennas* at the top and bottom of Map 28.